Numerical study of racking resistance of timber-made double-skin façade elements

Kozem Šilih, E.[a], **Premrov, M.**[a,*]

[a]University of Maribor, Faculty of Civil Engineering, Transportation Engineering and Architecture, Maribor, Slovenia

A B S T R A C T

The use of a double-skin façade (DSF) is a quite new approach in the building renovation process, complementing conventional renovation strategies. A double-skin façade is an envelope wall construction that consists of two transparent surfaces separated by a cavity and can essentially improve the thermal and acoustic resistance of the building envelope. The main double-skin wall components are usually composed of a hardened external single glazing pane and a double or triple thermal insulating internal glass pane, which are connected to the frame structure. Recently, many studies have analysed the thermal and acoustic performance of DSF elements, but almost none in terms of structural behaviour, especially in terms of determining the racking resistance of such wall elements. Moreover, with a view to reduce the global warming potential, an eco-friendly timber frame instead of a commonly used steel, aluminium or plastic frame is studied in this analysis. However, structurally combining timber and glass to develop an appropriate load-bearing structural element is a very complex process involving a combination of two materials with different material properties, where the type of bonding can be selected as a crucial parameter affecting the racking resistance range. Since the costs of experiments performed on such full-scale DSF elements are very high and such experiments are time-consuming, it is crucial to develop special mathematical models for analysing the influence of the most important parameters. Therefore, the main goal of this paper is to develop the finite element mathematical model of the studied DSF structural elements with a highly ecological solution by using a timber frame. In the second step, the developed model is further implemented in the numerical analysis of racking stiffness and followed by a comprehensive parametric numerical study on different parameters influencing the horizontal load-bearing capacity of such DSF timber elements. The obtained results indicate that the new approach of the developed load-bearing prefabricated timber DSF elements can essentially improve racking resistance and stiffness compared with the widely studied timber-glass single-skin wall elements and can thus be fully recommended especially in the structural renovation process of old buildings.

1. Introduction

In the past few decades, climate change has prompted experts to urgently call for action to remove the causes and alleviate the consequences of climate change that affect the environment, and design new buildings primarily with eco-friendly materials. Therefore, the field of energy consumption is witnessing a global trend aiming is to reduce greenhouse gas emissions. Consequently, a new strategy to design buildings with net zero emissions has to be adopted not only for new buildings, but also for building renovations, [1-4]. Since most energy flux is transmitted through

building envelope elements [5, 6], the façade upgrade with essential thermal transmittance decrease can be one of the most effective interventions to improve the thermal efficiency and aesthetic appeal of existing buildings, [4]. In this sense, the advantages of wood and glass have led to the development of so-called timber-glass wall elements, in which single-layer outer and thermal insulated inner double or triple glass panes are rigidly connected to the timber frame with a bonding line, [2, 4, 5]. Since such DSF wall elements were developed primarily as external building envelope elements to enhance solar heat gains of the building during the heating period, they are usually placed on the south façade of the building. The proper orientation of such transparent façade elements enables the utilisation of solar energy for heating and internal illumination of the building [7-11]. However, the consequent asymmetrical layout of such transparent wall elements can result in many problems with the horizontal stability of the whole building. Their asymmetrical position can cause a serious plan irregularity problem, which may result in high torsional actions caused by heavy seismic or wind loads. The contribution of such DSF wall elements to the horizontal carrying capacity of the whole building is usually neglected and has not yet been implemented in any standards.

Moreover, the hybrid steel-glass or timber-glass shear wall system can be created to realise hybrid structures with glass as the main stabilising material. Various hybrid glass component solutions are currently being studied mainly in the academic context, [12]. It was demonstrated in many experimental [4, 13, 14] and numerical studies [15] performed on full-scale single-skin timber-glass load-bearing structural wall elements that triple insulating glazing can foster higher racking resistance and stiffness compared with the single glazing. However, the racking stiffness is not in a range with the timber-framed walls with conventional sheathing boards, such as OSB or fibre-plaster boards, which are prescribed as primary load-bearing racking structural wall elements by standards. However, the goal of the design process in the comprehensive renovation of old buildings is also to improve the thermal standard of the building, and the sound and the racking resistance of the load-bearing envelope façade elements. Consequently, the concept of a specially developed double-skin façade (DSF) elements with an additional single-layer outer glass pane added to the commonly used triple insulating inner glazing rigidly connected to the frame structure and separated by a cavity could be a good and useful approach [16-18]. Such a solution can significantly decrease the U-value of such transparent envelope wall elements, and considerably improve the sound resistance.

Combining timber and glass to make an appropriate load-bearing structural element is a very complex process involving a combination of two materials with different material properties, where the bonding line can be selected as a crucial parameter affecting the obtained load-bearing range [14], [19-26]. It is important to point out that only the load-bearing approach to the racking resistance and stiffness of such timber DSF elements will be numerically analysed in this paper as an upgrade of the already published experimental [5, 13, 14] and numerical studies [15, 27] performed on full-scale timber-glass wall elements with double and triple insulating glazing, but only as a concept of single-skin façade (SSF) elements. No energy, LCA or acoustic studies on DSF elements will be performed in the presented study.

It should be emphasised that, to our knowledge, no special studies have been published on the topic of the racking resistance of timber DSF elements. In the broader study in [18], the structural approach to timber DSF was studied, but only for the vertical load impact. In [28], an experimental analysis of the racking resistance and stiffness of DSF elements was carried out as part of a national research project in two different specially selected full-scale test groups, varying the type of the adhesive connecting the insulating inner glazing to the timber frame (polyurethane and epoxy). As mentioned before, there are many different parameters which significantly influence the racking resistance and stiffness of timber DSF elements, especially the type of the bonding line between the glass pane and the timber frame, and the type and thickness of the glass panes. Since the experiments performed on such full-scale DSF elements are very time-consuming and also the costs are very high, it is crucial to develop special mathematical models to be used to further analyse the influence of most important parameters, and based on these results, to develop special simple final expressions for the racking resistance and stiffness of timber DSF elements to be suitable also for simple engineering usage.

The main goal of this paper is to develop a mathematical model of the studied DSF structural elements with a highly ecological solution by using a timber frame (Section 3). The developed finite element model can be further implemented in the numerical analysis of the racking resistance and stiffness (Section 4) and followed by a broad parametric numerical study on different most important parameters influencing the horizontal load-bearing capacity of such DSF elements (Section 5). Special attention will be dedicated to analysing the influence of the thickness t_a and width w_a of the bonding line, and to the thickness of the outer and inner glass pane t_{gl}. Based on our previous experimental [5, 13, 14, 25, 26] and numerical studies [15, 27] performed on conventional single-skin façade (SSF) timber-glass wall elements and certain findings from experiments performed on full-scale DSF elements [28], only a case with a polyurethane adhesive in the bonding line between the insulating inner glazing and the timber frame is analysed in the presented study as the most appropriate and useful bonding solution (Fig. 1).

2. Main concept of timber double-skin façade wall elements

According to [16], a double-skin façade (DSF) is an envelope element that consists of two transparent surfaces rigidly connected to a frame structure and separated by a cavity. The cavity is used as an air channel and can be naturally or mechanically ventilated and thus it does not offer an occupied space. The width of the cavity can vary from 200 mm to over 2 m. Solar shading systems can be integrated within the cavity. The insulating glazing is usually placed on the inner side of the façade, while the extra skin is placed on the external side to significantly improve the thermal transmittance of the wall element, and reduce the energy demand for heating and cooling, [16-18], [29-36]. The extra skin can reduce the cooling demand in the summer and the heating demand in the winter. Therefore, DSF elements have been proposed as a promising passive building technology to enhance energy efficiency and improve indoor thermal comfort [29]. Simulations of different envelope scenarios in the Mediterranean climate [36] have shown that the most energy efficient DSF is with low-e glazing as the outer layer. It is concluded in [17], however, that in warm climates its benefit in the summer is limited. Such a constructed envelope element also demonstrates better sound resistance [29, 35, 36] in comparison with widely used SSF elements and can, therefore, be suitable for high noise areas where a high level of sound insulation is required.

The exterior glazing primarily consists of a hardened fully tampered single glass pane, while ordinary annealed glass is usually used for the thermal-insulating double or triple inner glazing, as schematically presented in Fig. 1. As already mentioned in the introduction, the type of the bonding line with appropriate adhesive dimensions was the crucial parameter in the structural behaviour of experimentally and numerically tested single-skin timber-glass façade wall elements against a horizontal load impact. Additionally, there are many types of adhesives to choose from, such as silicone, polyurethane, acrylate and epoxy.
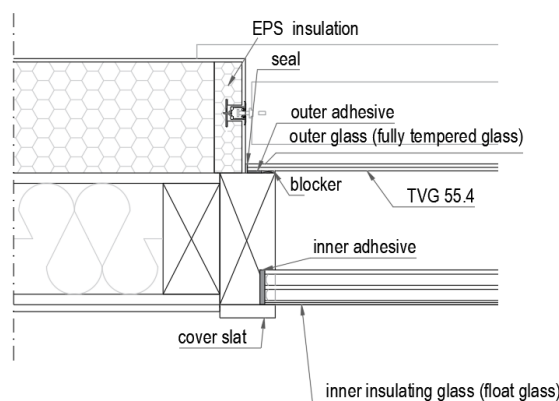

Fig. 1 Schematic presentation of the timber DSF wall element

Basically, the frame structure can be made from many different materials, but it is mainly made from steel, aluminium or plastic. However, it is obvious that, for this specific building typology to reach the zero energy building targets, mere energy conserving strategies involving decreases with the DSF elements energy demand for heating and cooling, as stated before, may not suffice. Renewable energy sources and technologies should be additionally considered as integral parts of the building envelope and systems [36]. Bearing in mind an eco-friendly renovation approach, the use of low-carbon materials is one of the most acknowledged mitigation measures for carbon reduction. Therefore, the adoption of timber as the main structural frame material can potentially further reduce the overall embodied carbon, [18]. Consequently, our study will be limited to the approach using a timber frame.

In addition to the foreseen structural advantages, the DSF envelope wall elements improve the sound insulation of the building envelope and energy performance compared to the regular triple insulating glazing [17, 18, 29], therefore they can be very useful especially in renovation process by upgrading of the envelope elements in old existing buildings, compared also with commonly used single-skin façade solutions. However, most studies do not address structural solutions, instead focusing on energy analyses and their impact on the LCA results or analyses of sound insulation compared to single façade transparent elements. The numerical study in [18] is focused only on the vertical load impact but does not address the racking resistance range as the most important if the DSF elements are considered bracing structural elements.

3. Mathematical model

The studied DSF wall elements have been modelled and analysed by using the commercial finite element model (FEM) computer program SAP2000 Nonlinear v 17.0.0 [37]. In the computational model, the timber frame was modelled by 1-dimensional (beam) finite elements, while the glazing boards were modelled using 2-dimensional finite elements of the "composite shell" type, which allows for the simulating of composite multi-layer shells. The adhesive bonding of the glazing panes to the timber frame was modelled using linear link elements (springs). As in reality, the adhesive bonding is provided continuously over the whole perimeter, the stiffness properties of the discrete spring elements were defined based on the spacing of the springs in the computational model using Eqs. 1 and 2 [15, 22, 38] for the inner and outer type of the bonding line:

$$K_1 = \frac{E_a \cdot A_a}{t_a} = \frac{E_a \cdot (w_a \cdot l_a)}{t_a} \tag{1}$$

$$K_2 = \frac{G_a \cdot A_a}{t_a} = \frac{G_a \cdot (w_a \cdot l_a)}{t_a} \tag{2}$$

where K_1 is the stiffness in the direction normal to the connected plane, while K_2 is the shear stiffness in the two perpendicular directions in the connected plane. E_a and G_a are the modulus of elasticity and the shear modulus of the adhesive material, respectively, t_a and w_a designate the thickness and the width of the adhesive layer, respectively, while l_a is the impact length for a single spring element and is equal to the spacing between the springs. According to the scheme in Fig. 2b in our study, the bonding line between the inner glazing and the timber frame is marked with $t_{a,inn}$ and $w_{a,inn}$ variable parameters for the springs in Eqs. 1 and 2, while the parameters $t_{a,out}$ and $w_{a,out}$ are used for the outer bonding in the modelling process.

The present study was performed for the case of the double-skin timber-glass wall system DSF-P (double-skin façade) with full-scale dimensions of 1.25 m × 2.34 m (Fig. 2a), taken from the experimental analysis performed in [28]. The geometry and the typical cross-section of the DSF wall element with all adhesive types are shown in Fig. 2. As stated, two different types of adhesives were used, i.e. polyurethane (Ködiglaze P, [39]) for the inner triple insulation glazing, and silicone (Ködiglaze S, [40]) for the outer single glazing. The timber frame is composed of glue-laminated timber GL24h according to the EN 1194 classification [41]. For the inner triple insulating glazing, float glass (44.2) is used [42], i.e. glass panes 2, 3 and 4 in Fig. 2b, while a thermally toughened soda lime silicate safety glass (TVG 55.4) is used for the single outer glazing [43], i.e. glass pane 1 in Fig. 2b. It is important to point out that only the linear-elastic behaviour of all material components will be considered at this stage of modelling.
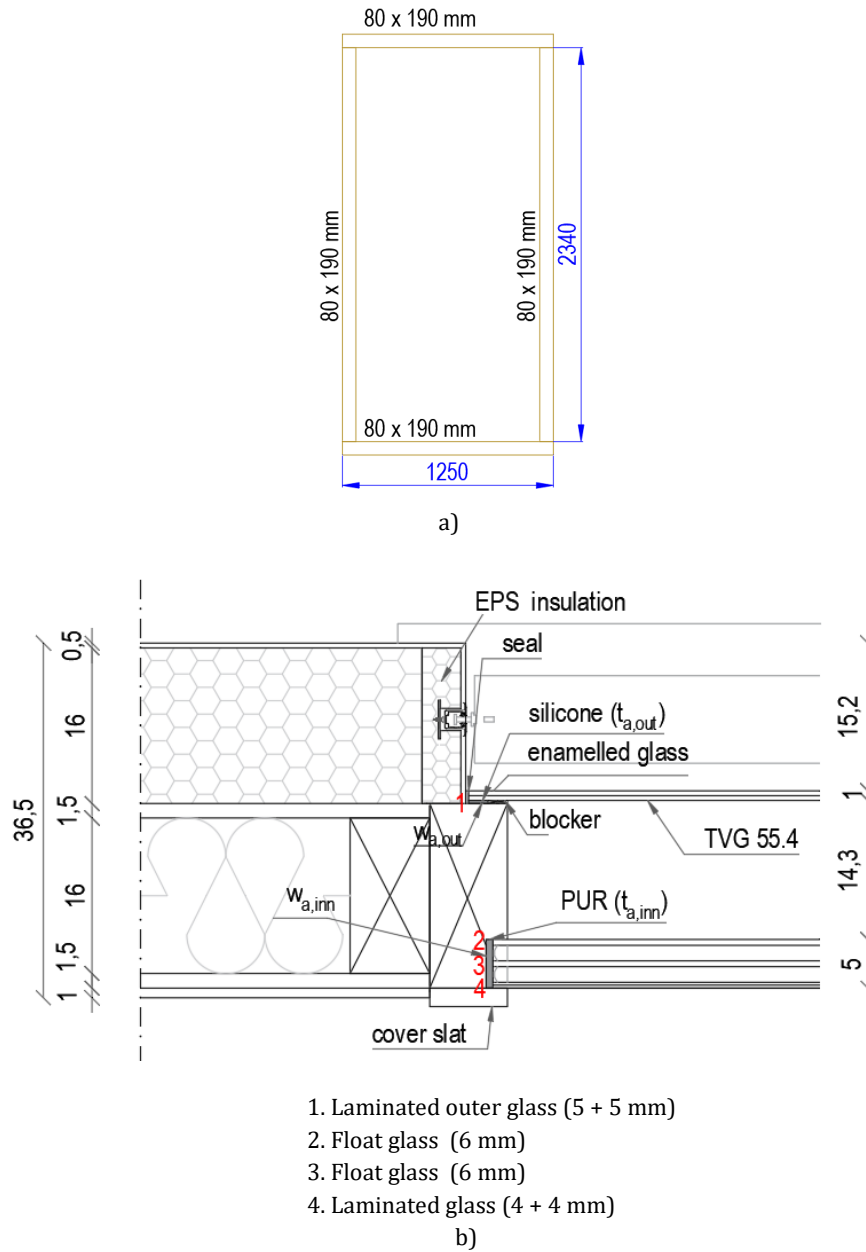
a)

1. Laminated outer glass (5 + 5 mm)
2. Float glass (6 mm)
3. Float glass (6 mm)
4. Laminated glass (4 + 4 mm)

b)

Fig. 2 External dimensions of the wall samples and dimensions of the timber frame elements (a), and the system cross-section with installation details (b)

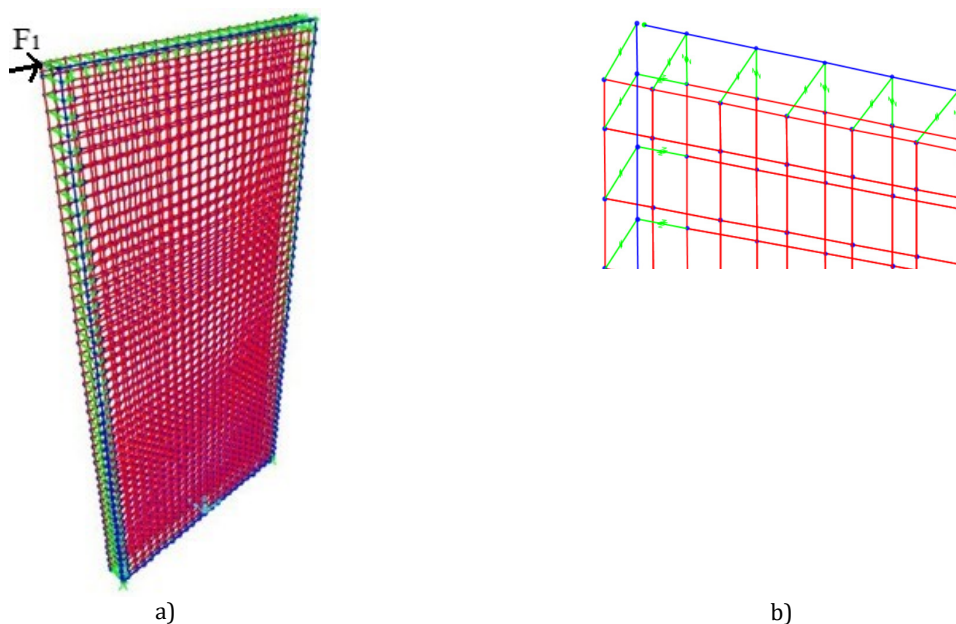**Table 1** Material properties of the adhesives [39, 40]

	Poisson's ratio ν	Shear modulus G_s (MPa)	Elastic modulus E_0 (MPa)	Decay time t_d (s)	Decay constant β
Silicone (Ködiglaze S)	0.5	0.351	1,053	100	0.0026
Polyurethane (Ködiglaze P)	0.49	0.454	1,354	290	0.0016

The input data for two types of adhesives, and the material properties of the glass and timber are listed in Tables 1 and 2, respectively.

Table 2 Material properties of the timber [41] and glass components [42, 43]

	Timber frame GL24h [41]		Float glass [42]	Thermally toughened glass [43]
Standard	EN 1194		EN 12150	EN 12150
E (MPa)	II 11,600	⊥ 720	70,000	70,000
ν (-)	II 0.25	⊥ 0.45	0.23	0.23
G (MPa)	II 720	⊥ 35	0.45	0.45
f_t (MPa)	II 14	⊥ 0.5	45	120
f_c (MPa)	II 14	⊥ 0.5	500	500
ρ (kg/m³)	380		2,500	2,500

The developed numerical finite element model of the whole composite DSF wall element as established in SAP 2000 [37] is shown in Fig. 3a. The timber material was considered as an isotropic elastic material (with the modulus of elasticity $E_{0,mean}$) and the elements of the timber frame were modelled as the simple plane-stress elements. Both glass panes were modelled using the linear shell elements offered by the SAP2000 software. While glass is a very brittle material it was therefore modelled as acting linearly elastic in tension and compression. The schematic presentation of the detail bonding line modelling simulating the adhesive bonding between the timber frame and both glazings by using discrete two-dimensional spring elements with perpendicular stiffness properties K_1 and K_2 is presented in Fig. 3b. It is important to point out that the bonding lines for the outer and inner glazing are modelled and simulated separately with different values of K_1 and K_2 according to Eqs. 1 and 2. The tensile (left bottom) support was arranged using three M16 bolts and two steel plates (one on each side of the wall element). The steel plates were connected to a rigid steel frame. In the numerical model, the bolts were considered as linear elastic spring supports with the stiffness equal to the slip modulus K_{ser} for bolts. It should be noted that the steel plates were not included in the numerical model. The compressive (right bottom) support was modelled using rigid point supports.

a)   b)

Fig. 3 a) DSF-P finite element model, and b) the presentation of the spring/link elements

4. Numerical analysis and discussion of results

In the numerical analysis, the model was loaded with a vertical load in the first phase, followed by the second phase with a gradual increase of the horizontal load ("step by step analysis"). Based on the ratio between the horizontal force and the calculated displacement, the racking stiffness R was determined. Subsequently, the results were compared with the results of the experimental tests performed in [28].

Fig. 4 shows a comparison between the results of the experimental tests [28] performed on three full-scale test samples with the polyurethane adhesive for the inner glazing (DSF-P1, DSF-P2 and DSF-P3) and the numerical analysis performed on the test samples with exactly the same all dimensions presented in Fig. 2 and all material properties listed in Tables 1 and 2.

The diagram shows a very good agreement between the numerical and experimental results of three full- scale test samples regarding the behaviour of the structure in the elastic range until irreversible non-linear deformations appear. However, it should be mentioned that the test samples in [28] were experimentally tested pending the total failure of the element and the yielding of both adhesives occurred by the forces of approximately F_1 = 28 kN. This yielding stage of the adhesive was not modelled with our developed mathematical model, as in the first phase of the developed new structural DSF elements, it is assumed to be used only as a bracing element for buildings, where the wind load is decisive as the horizontal load impact and the structure thus has to be dimensioned only in the linear-elastic range.

The horizontal displacement u_1 at a force of F_1 = 10 kN and the calculated racking stiffness R for both experimental test and the numerical simulation are presented in Table 3. For the experimental results, the average value of all three test samples is calculated [28].

It is obvious from the presented results that the numerical results exhibit a very good agreement with the experimental ones. Therefore, it can be concluded that the developed FE model can be used for further parametrical studies with different parameters, which can significantly affect the racking resistance of DSF wall elements.
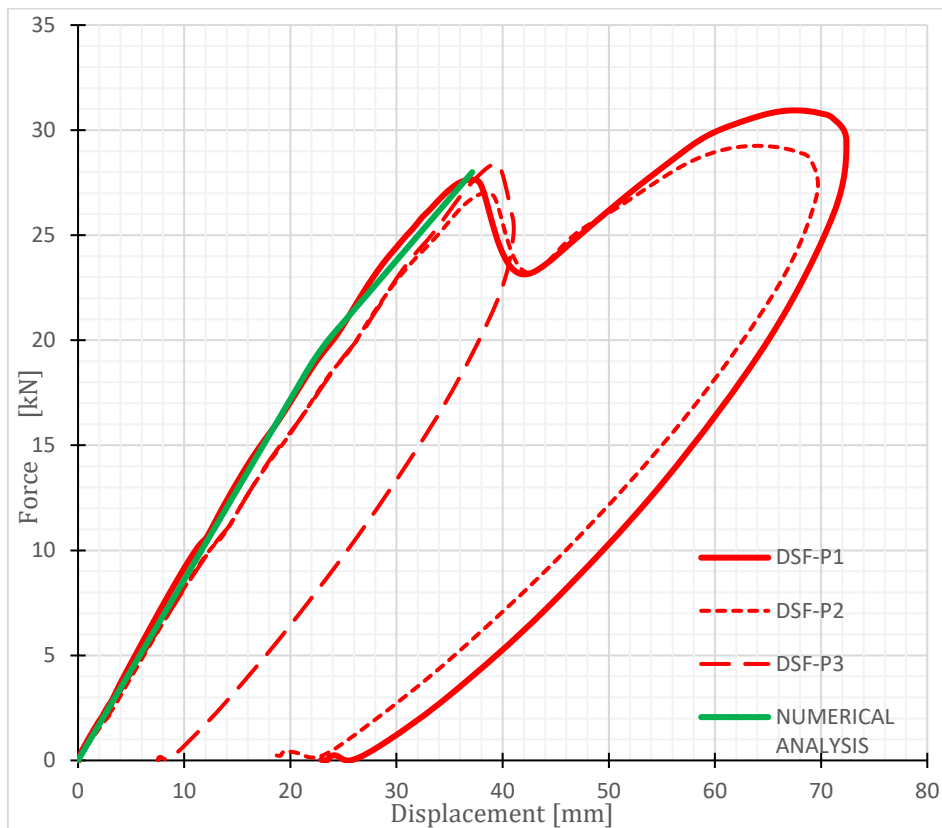

Fig. 4 Experimental and numerical force-displacement diagrams for the DSF-P wall element

Table 3 Experimental and numerical displacements at an acting force of F_1 = 10 kN and racking stiffness R

Model type	DSF-P
Displacement u_1 (mm) at F_1 = 10 kN – numerical	11.67
Displacement u_1 (mm) at F_1 = 10 kN – experimental [28]	11.00
Numerical stiffness: $R = F_1 / u_1$ (N/mm)	857
Experimental stiffness [28]: $R = F_1 / u_1$ (N/mm)	909

5. Parametric numerical analysis of the horizontal load-bearing capacity and stiffness of DSF-P wall elements

The parametric analysis was performed on the DSF-P model, in which the polyurethane adhesive thickness of the inner insulating glazing $t_{a,inn}$ was varied first, while the other parameters, such as silicone adhesive thickness of the outer glazing, glass thickness t_{gl} and the width of the adhesive layer w_a, remained unchanged. The thickness of the outer single glass (Glass 1) and the thickness of the triple inner insulating glass (Glass 2, 3, 4) according to Fig. 2b were further varied. In this case, the widths of the adhesive layer changed depending on the thickness of Glasses 2 and 3.

5.1 Analysis of the influence of the adhesive thickness on the horizontal load-bearing capacity of DSF wall panels

In the first parametric study, the thickness of the polyurethane adhesive bonding the triple insulating glazing to the timber frame was parametrically changed ($t_{a,inn}$ = 3 mm, 5 mm, 7 mm, 9 mm), while the thickness of the silicone bonding the outer glass pane to the timber frame was constant $t_{a,out}$ = 3 mm in all cases.

Table 4 and Fig. 5 show the results of displacements at an acting horizontal force of F_1 = 10 kN and the calculated racking stiffness as a function of the thickness of the variable polyurethane adhesive.

As expected, the racking stiffness of the wall element almost hyperbolically decreases with the increasing thickness of the polyurethane adhesive, since a greater thickness of adhesive represents a greater yielding of the joint between the timber frame and the glass. Very similar conclusions on the influence of the adhesive thickness were also obtained in the numerical study in [15] performed on single-skin façade elements with only triple or double insulating glazing.

Table 4 Displacements u and stiffnesses R at different thicknesses of the polyurethane adhesive $t_{a,inn}$

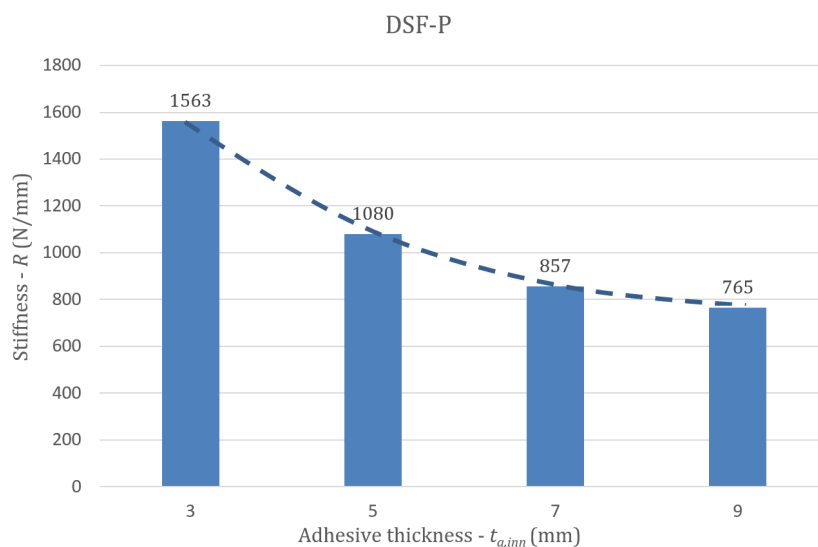| $t_{a,inn}$ (mm)	u at F_1 = 10 kN (mm)	R (N/mm)
3	6.40	1,563
5	9.26	1,080
7	11.67	857
9	13.07	765

Fig. 5 Racking stiffness values for the parametrical selected adhesive thicknesses $t_{a,inn}$

5.2 Analysis of the influence of the glass thickness on the horizontal load-bearing capacity of DSF wall elements

Parametric analyses were also carried out, varying the thickness of the outer Glass 1 $t_{gl,out}$ and of the inner glasses 2, 3, 4 $t_{gl,inn}$ and taking into account the respective constant width of the polyurethane adhesive layer w_a = 28 mm for the inner glazing. The layout of the glasses is shown in Fig. 6.

Table 5 shows the results for different thicknesses of the outer single Glass 1 $t_{gl,out}$ at an acting horizontal force of F_1 = 10 kN with a constant adhesive thickness of $t_{a,inn}$ = 7 mm and width $w_{a,out}$ = 20 mm for the fixing of the triple inner insulating glass to the timber frame. The silicone adhesive of the constant thickness of $t_{a,out}$ = 3 mm was used to fix the single outer insulating glass to the timber frame. The thicknesses of the inner triple glazing (Glasses 2, 3, 4) are constant and the same as used in the experimental analysis [28].

It is evident from the listed results that the glass thickness $t_{gl,out}$ has almost no impact on the racking resistance if the width of the bonding line $w_{a,out}$ is not adequately changed. Therefore, the width of the adhesive in the bonding line w_a will be systemically changed with the increasing thickness of the glass panes t_{gl} in our further analysis.
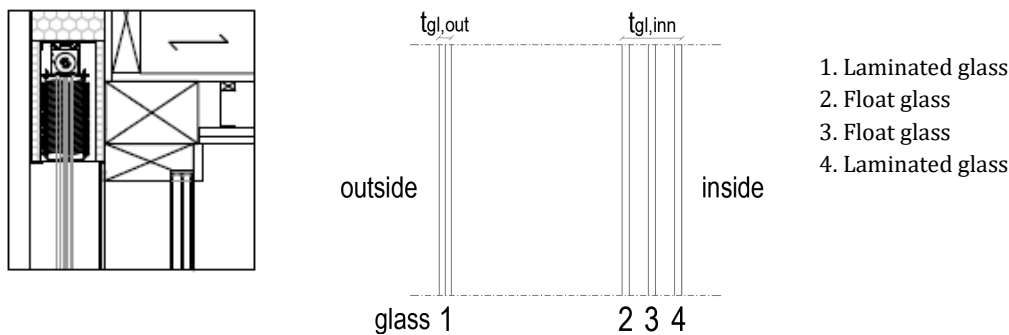

Fig. 6 Illustration of the glass layout and thickness of the DSF-P wall element

Table 5 Calculated displacements u and stiffness R for different glass thicknesses of outer Glass 1 $t_{gl,out}$

Glass pane	Thicknesses of the outer glass $t_{gl,out}$ and inner glass $t_{gl,inn}$ (mm)			
	Example 1	Example 2	Example 3	Example 4
1 – outer	4 + 4	5 + 5	6 + 6	7 + 7
$w_{a,out}$ (mm)	20	20	20	20
2 – inner	6	6	6	6
3 – inner	6	6	6	6
4 – inner	4 + 4	4 + 4	4 + 4	4 + 4
u (mm) at F_1 = 10 kN	11.68	11.67	11.66	11.64
R (N/mm)	856.16	856.90	857.63	859.11

5.3 Analysis of the influence of the adhesive layer width on the horizontal load-bearing capacity of DSF wall elements
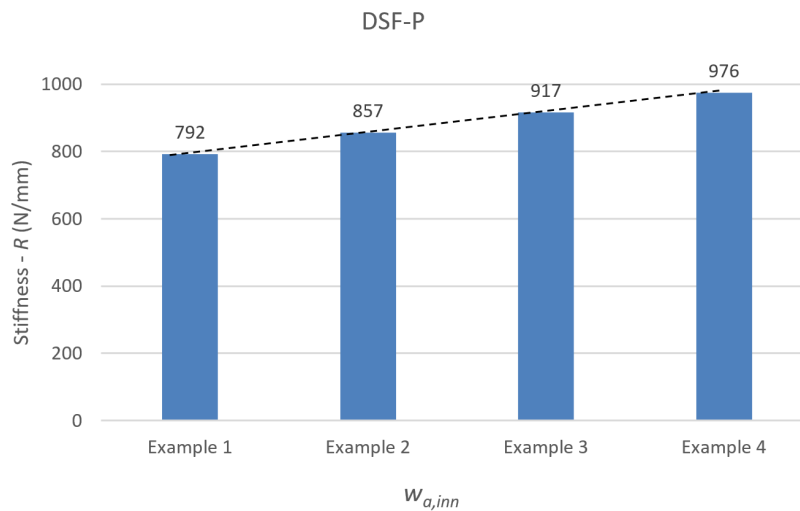
Table 6 shows the obtained numerical results for different parametrically selected thicknesses of the triple inner insulating glass (glasses 2, 3, 4) at an acting force of F_1 = 10 kN. The inner glazing is bonded to the timber frame with a polyurethane adhesive with a constant thickness of $t_{a,inn}$ = 7 mm. The thickness of the silicone adhesive fixing of the outer single glass (Glass 1) to the timber frame remained unchanged $t_{a,out}$ = 3 mm and the thickness of the outer Glass 1 $t_{gl,out}$ remained constant (5 + 5 mm) as used in the experimental study [28].

The calculation of the spring stiffness takes into account the influence of the adhesive layer width w_a and varies according to the thickness of glasses 2, 3 and 4. Consequently, the values $w_{a,inn}$ systematically increase from 24 mm in Example 1 to 36 mm in Example 4.

The calculated results are graphically presented in Fig. 7. The linear approximation is marked with the dashed line.

Table 6 Displacements u and stiffness R for different glass thicknesses 2, 3, 4

Glass pane	Thicknesses of the outer glass $t_{gl,out}$ and inner glass $t_{gl,inn}$ (mm)			
	Example 1	Example 2	Example 3	Example 4
1 – outer	5 + 5	5 + 5	5 + 5	5 + 5
2 – inner	4	6	8	10
3 – inner	4	6	8	10
4 – inner	3 + 3	4 + 4	5 + 5	6 + 6
$w_{a,inn}$ (mm)	24	28	32	36
u (mm) at F_1 = 10 kN	12.62	11.67	10.90	10.25
R (N/mm)	792	857	917	976

Fig. 7 Stiffness for different cases of the considered width of the adhesive

The results evidently demonstrate that the thickness of the outer single Glass 1 has practically no influence on the racking stiffness of the wall element if the corresponding width of the adhesive is not changed. On the other hand, increasing the thickness of the inner insulating glasses 2, 3 and 4, but considering the corresponding increasing width of the adhesive layer w_a in Eqs. 1 and 2, increases the overall DSF racking stiffness in an almost linear way, and has an important positive effect on the horizontal load-bearing capacity of the wall element.

6. Conclusion

The paper presents the finite element model developed and used for the numerical analysis of the resistance and stiffness of double-skin façade (DSF) elements. Respecting the known facts from different experimental and numerical analyses performed on single-skin timber-glass wall elements, there are many various parameters which significantly affect the racking resistance of such elements and can be further implemented to double-skin timber glass façade elements. Considering that the costs of the experiments performed on such full-scale DSF elements are very high and such experiments are time-consuming, an extensive parametric numerical study of various main parameters influencing the horizontal load carrying capacity of such DSF elements was performed. Particular attention was paid to the analysis of the influence of the adhesive thickness and the width of the bonding line as well as the thickness of the outer and inner glazing panel.

The computational analyses carried out on individual load-bearing DSF wall elements have shown a considerable influence of the adhesive layer width bonding the glass pane to the timber frame with almost linear behaviour approximation (Fig. 7), while the second important parameter, i.e. the adhesive thickness, exhibited almost hyperbolical influence (Fig. 5). On the other hand, the glass thickness was found to be a less important parameter, which becomes relevant only if the width of the adhesive layer increased simultaneously and adequately with the glass thickness.

The obtained results indicate that the new approach of the developed load-bearing prefabricated timber DSF elements can essentially improve racking resistance and stiffness compared

with the widely studied timber-glass single-skin wall elements and can thus be fully recommended especially in the structural renovation process of old buildings.

However, the presented spring FE model is maybe still complex for practical engineering usage, but very useful for parametrical research studies. Therefore, our future work will be focused to development of a simple mathematical model with fictive diagonals [27] also for DSF elements to be used in simple computational FEM programs. Due to its simplicity such a model than it can be used for modelling with simpler and cheaper programs.

References

[1] Jensen, P.A., Maslesa, E., Berg, J.B., Thuesen, C. (2018). 10 questions concerning sustainable building renovation, *Building and Environment*, Vol. 143, 130-137, doi: 10.1016/j.buildenv.2018.06.051.

[2] Abdul Hamid, A., Farsäter, K., Wahlström, Å., Wallentén, P. (2018). Literature review on renovation of multifamily buildings in temperate climate conditions, *Energy and Buildings*, Vol. 172, 414-431, doi: 10.1016/j.enbuild.2018.04.032.

[3] Ascione, F., Bianco, N., De Masi, R.F., Mauro, G.M., Vanoli, G.P. (2017). Energy retrofit of educational buildings: Transient energy simulations, model calibration and multi-objective optimization towards nearly zero-energy performance, *Energy and Buildings*, Vol. 144, 303-319, doi: 10.1016/j.enbuild.2017.03.056.

[4] Žegarac Leskovar, V., Premrov, M. (2019). *Integrative approach to comprehensive building renovations*, Springer, Cham, Switzerland, doi: 10.1007/978-3-030-11476-3.

[5] Žegarac Leskovar, V., Premrov, M. (2013). *Energy-efficient timber-glass houses*, Springer, London, United Kingdom doi: 10.1007/978-1-4471-5511-9.

[6] Rules on efficient use of energy in buildings (2010). Official Gazette, Republic of Slovenia, 52/2010, from *http://www.pisrs.si/Pis.web/pregledPredpisa?id=PRAV14331*, accessed November 13, 2021.

[7] Inanici, M.N., Demirbilek, F.N. (2000). Thermal performance optimization of building aspect ratio and south window size in five cities having different climatic characteristic of Turkey, *Building and Environment*, Vol. 35, No. 1, 41-52, doi: 10.1016/S0360-1323(99)00002-5.

[8] Chiras D. (2002). *The solar house: Passive heating and cooling*, Chelsea Green Publishing, White River Junction, Vermont, USA.

[9] Persson, M.-L., Roos, A., Wall, M. (2006). Influence of window size on the energy balance of low energy houses, *Energy and Buildings*, Vol. 38, No. 3,181-188, doi: 10.1016/j.enbuild.2005.05.006.

[10] Hachem, C., Athientis, A., Fazio, P. (2011). Parametric investigation of geometric form effects on solar potential of housing units, *Solar Energy*, Vol. 85, No. 9, 1864-1877, doi: 10.1016/j.solener.2011.04.027.

[11] Premrov, M., Žigart, M., Žegarac Leskovar, V. (2018). Influence of the building shape on the energy performance of timber-glass buildings located in warm climatic regions, *Energy*, Vol. 149, 496-504, doi: 10.1016/j.energy.2018.02.074.

[12] Feldmann, M., Kasper, R., Abeln, B., Cruz, P., Belis, J., Beyer, J., Colvin, J., Ensslen, F., Eliasova, M., Galuppi, L., Gessler, A., Grenier, C., Haese, A., Hoegner, H., Kruijs, R., Lanosch, K., Louter, C., Manara, G., Morgan, T., Neugebauer, J., Rajcic, V., Royer-Carfagni, G., Schneider, J., Schula, S., Siebert, G., Sulcova, Z., Wellershoff, F., Zarnic, R. (2014). *Guidance for European structural design of glass components*, European Commission, Joint Research Centre, Institute for the Protection and Security of the Citizen, Ispra, Italy.

[13] Premrov, M., Dujič, B., Ber, B. (2013). Glazing influence on the seismic resistance of prefabricated timber-framed buildings, In: Belis, J., Louter, C. (eds.), *COST action TU0905 mid-term conference on structural glass*, CRC Press, Boca Raton, Florida, USA, 25-32.

[14] Premrov, M., Serrano, E., Winter, W., Fadai, A., Nicklisch, F., Dujič, B., Sustersic, I., Brank, B., Strukelj, A., Drzecnik, M., Buyuktaskin, H.A., Erol, G., Ber, B. (2015). Workshop report *WP 6: Testing on life-size specimen components: shear walls, beams and columns including long-term behaviour*: WoodWisdom-net, research project, load bearing timber-glass-composites, 2012-2014, 15.

[15] Ber, B., Finžgar, G., Premrov, M., Štrukelj, A. (2018). On parameters affecting the racking stiffness of timber-glass walls, *Glass Structures & Engineering,* No. 4, 69-82, doi: 10.1007/s40940-018-0086-5.

[16] Saelens, D. (2002). *Energy performance assessment of single-storey multiple-skin facades*, Catholic University of Leuven, Belgium, PhD Dissertation, from *https://bwk.kuleuven.be/bwf/PhDs/PhDSaelens*, accessed November 15, 2021.

[17] Alibaba, H.Z., Ozdeniz, M.B. (2016). Energy performance and thermal comfort of double-skin and single-skin facades in warm-climate offices, *Journal of Asian Architecture and Building Engineering*, Vol. 15, No. 3, 635-642, doi: 10.3130/jaabe.15.635.

[18] Pomponi, F., D´Amico, B. (2017). Holistic study of a timber double skin façade: Whole life carbon emissions and structural optimization, *Building and Environment*, Vol. 124, 42-56, doi: 10.1016/j.buildenv.2017.07.046.

[19] Niedermaier, P. (2003). Shear-strength of glass panel elements in combination with timber frame constructions, In: *Proceedings of the 8th International Conference on Architectural and Automotive Glass (GPD)*, Tampere, Finland, 262-264.

[20] Cruz, P.J.S., Pacheco, J.A.L., Pequeno, J.M.B. (2007). Experimental studies on structural timber glass adhesive bonding, In: *COST E34, Bonding of Timber, 4th Workshop »Practical Solutions for Furniture & Structural Bonding,* Larnaca, Cyprus, 67-75.

[21] Neubauer, G., Schober, P. (2008*). Holz-Glas-Verbundkonstruktionen*, Weiterentwicklung und Herstellung von Holz-Glas-Verbundkonstruktionen durch statisch wirksames Verkleben von Holz und Glas zum Praxiseinsatz im Holzhausbau (Impulsprojekt V2 des Kind Holztechnologie), Endbericht, Holzforschung Austria, Vienna, Austria.

[22] Hochhauser, W. (2011). *A contribution to the calculation and sizing of glued and embedded timber-glass composite panes,* PhD Thesis*,* Vienna University of Technology, Austria.

[23] Blyberg, L. (2011). *Timber/glass adhesive bonds for structural applications*, Licentiate thesis, Linnaeus University, School of Engineering, Växjö, Sweden, from *http://www.diva-portal.org/smash/get/diva2:447937/FULL TEXT01.pdf*, accessed November 15, 2021.

[24] Blyberg, L., Serrano, E., Enquist, B., Sterley, M. (2012). Adhesive joints for structural timber/glass applications: Experimental testing and evaluation methods, *International Journal of Adhesion and Adhesives*, Vol. 35, 76-87, doi: 10.1016/j.ijadhadh.2012.02.008.

[25] Ber, B., Premrov, M., Štrukelj, A., Kuhta, M. (2014). Experimental investigations of timber-glass composite wall panels, *Construction and Building Materials*, Vol. 66, 235-246, doi: 10.1016/j.conbuildmat.2014.05.044.

[26] Štrukelj, A., Ber, B., Premrov, M. (2015). Racking resistance of timber-glass wall elements using different types of adhesives, *Construction and Building Materials*, Vol. 93, 130-143, doi: 10.1016/j.conbuildmat.2015.05.112.

[27] Premrov, M., Ber, B., Kozem Šilih, E. (2021). Study of load-bearing timber-wall elements using experimental testing and mathematical modelling, *Advances in Production Engineering & Management*, Vol. 16, No. 1, 67-81, doi: 10.14743/apem2021.1.385.

[28] Premrov, M., Zegarac Leskovar, V., Ber, B., Kozem Silih, E., Vogrinec, K., Lesnik, M. (2021). *Razvoj multifunkcijskega klimatsko aktivnega nosilnega ovoja objektov - DOM+: zaključno poročilo raziskovalnega projekta: delovni paket A1.2 Raziskava nosilnosti in togosti DSF stenskih elementov* (UM FGPA, TRL 3-4): trajanje projekta (TRL 3-4): 1. 3. 2019-28. 2. 2021. Maribor: Univerza v Mariboru, Fakulteta za gradbeništvo, prometno inženirstvo in arhitekturo, Slovenia.

[29] Ghaffarianhoseini, A., Ghaffarianhoseini, A., Berardi, U., Tookey, J., Li, D.H.W., Kariminia, S. (2016). Exploring the advantages and challenges of double-skin facades (DSFs), *Renewable and Sustainable Energy Reviews*, Vol. 60, 1052-1065, doi: 10.1016/j.rser.2016.01.130.

[30] Poirazis, H. (2004). *Double skin façades for office buildings*, Literature review, Department of Construction and Architecture, Lund University, Lund, Sweden.

[31] Xu, L., Ojima, T. (2007). Field experiments on natural energy utilization in a residential house with a double skin façade system, *Building and Environment*, Vol. 42, No. 5, 2014-2023, doi: 10.1016/j.buildenv.2005.07.026.

[32] Chan, A.L.S., Chow, T.T., Fong, K.F., Lin, Z. (2009). Investigation on energy performance of double skin façade in Hong Kong, *Energy and Buildings*, Vol. 41, No. 11, 1135-1142, doi: 10.1016/j.enbuild.2009.05.012.

[33] Haase, M., Marques da Silva, F., Amato, A. (2009). Simulation of ventilated facades in hot and humid climates, *Energy and Buildings*, Vol. 41, No. 4, 361-373, doi: 10.1016/j.enbuild.2008.11.008.

[34] Tijjani Musa, B., Alibaba, H.Z. (2016). Evaluating the use of double skin facade systems for sustainable development, *International Journal of Recent Research in Civil and Mechanical Engineering*, Vol. 2, No. 2, 151-159.

[35] Huckemann, V., Borges Leão, É., Leão, M. (2009). Acoustic comfort in office buildings with double skin glass façades, *Bauphysik*, Vol. 31, No. 5, 305-312, doi: 10.1002/bapi.200910040.

[36] Saroglou, T., Theodosiou, T. Givoni, B., Meir, I.A. (2019). A study of different envelope scenarios towards low carbon high-rise buildings in the Mediterranean climate - can DSF be part of the solution?, *Renewable and Sustainable Energy Reviews*, Vol. 113, Article No. 109237, doi: 10.1016/j.rser.2019.06.044.

[37] CSI. SAP2000 (v17.0.0). (2010). *Linear and nonlinear static and dynamic analysis and design of three-dimensional structures.* Berkeley: Computer & Structures, Inc.

[38] Kreuzinger, H., Niedermaier, P. (2005). *Glas als Schubfeld*, Tagungsband Ingenieurholzbau, Karlsruher Tage.

[39] Kömmerling, Product Information Ködiglaze P (2008). Special adhesive for bonding insulating glass units into the window sash.

[40] Kömmerling, Product Information Ködiglaze S (2008). Special adhesive for structural and direct glazing.

[41] European Committee for Standardization, (2003). EN 1194:2003: Timber structures – glued laminated timber strength classes and determination of characteristic values, Brussels.

[42] European Committee for Standardization, (2004). EN 572-2:2004: Glass in building – Basic soda lime silicate glass products – Part 2: Float glass, Brussels.

[43] European Committee for Standardization, (2000). EN 12150-1:2000: Glass in building – Thermally toughened soda lime silicate safety glass – Part 1: Definition and description, Brussels.